ELSEVIER

Biomaterials 23 (2002) 193–202

Biomaterials

www.elsevier.com/locate/biomaterials

Calcium phosphate cement containing resorbable fibers for short-term reinforcement and macroporosity

Hockin H.K. Xu*, Janet B. Quinn

Paffenbarger Research Center, American Dental Association Health Foundation, National Institute of Standards and Technology, Building 224, Room A-153, Gaithersburg, MD 20899, USA

Received 6 November 2000; received in revised form 8 February 2001; accepted 6 March 2001

Abstract

Calcium phosphate cement (CPC) sets to form hydroxyapatite and has been used in medical and dental procedures. However, the brittleness and low strength of CPC prohibit its use in many stress-bearing locations, unsupported defects, or reconstruction of thin bones. Recent studies incorporated fibers into CPC to improve its strength. In the present study, a novel methodology was used to combine the reinforcement with macroporosity: large-diameter resorbable fibers were incorporated into CPC to provide short-term strength, then dissolved to create macropores suitable for bone ingrowth. Two types of resorbable fibers with 322 μm diameters were mixed with CPC to a fiber volume fraction of 25%. The set specimens were immersed in saline at 37°C for 1, 7, 14, 28 and 56 d, and were then tested in three-point flexure. SEM was used to examine crack-fiber interactions. CPC composite achieved a flexural strength 3 times, and work-of-fracture (toughness) nearly 100 times, greater than unreinforced CPC. The strength and toughness were maintained for 2–4 weeks of immersion, depending on fiber dissolution rate. Macropores or channels were observed in CPC composite after fiber dissolution. In conclusion, incorporating large-diameter resorbable fibers can achieve the needed short-term strength and fracture resistance for CPC while tissue regeneration is occurring, then create macropores suitable for vascular ingrowth when the fibers are dissolved. The reinforcement mechanisms appeared to be crack bridging and fiber pullout; the mechanical properties of the CPC matrix also affected the composite properties.

Keywords: Calcium phosphate cement; Hydroxyapatite; Resorbable fiber; Reinforcement; Strength; Macroporosity

1. Introduction

The need for biomaterials in dental, craniofacial and orthopaedic applications has increased as the world population ages [1–3]. Due to their osteoconductivity and bone replacement capability, calcium phosphate cements are highly promising for use in a wide range of applications [4–7]. Several formulations of calcium phosphate cements self-harden through a setting reaction that forms hydroxyapatite [4–7]. One such cement [5], comprising of a mixture of fine particles of tetracalcium phosphate (TTCP: $Ca_4(PO_4)_2O$) and dicalcium phosphate anhydrous (DCPA: $CaHPO_4$), reacts in an aqueous environment at room or body temperature to form hydroxyapatite as the principal reaction product [8–13]. This calcium phosphate cement will be referred to as CPC. The CPC powder can be mixed with water to form a paste that can be sculpted during surgery, and within about 15 min this paste converts in situ to microporous solid crystalline hydroxyapatite [10,14]. CPC has excellent biocompatibility and bone-replacing properties and has been studied extensively [5–13]. Previous studies have suggested it to be useful in a number of medical and dental procedures, including the reconstruction of frontal sinus and augmentation of craniofacial skeletal defects [13,15–19], endodontics [20–22], and the repair of periodontal bone defects and tooth defects [23,24]. However, the relatively low strength and susceptibility to brittle catastrophic fracture of the cement have severely limited its use to only non load-bearing applications [9,11,13,17–19,23,24]. The use of the cement "is limited to the reconstruction of

*Corresponding author. Tel.: +1-301-975-6804; fax: +1-301-963-9143.

E-mail address: hockin.xu@nist.gov (H.K. Xu).

0142-9612/02/$ - see front matter
PII: S0142-9612(01)00095-3

non-stress-bearing bone" [18], and "clinical usage was limited by...brittleness..." [8].

Fibers are widely used to improve the strength and fracture resistance of materials [19,25–31]. Poly(methyl methacrylate) bone cements have been reinforced with carbon fibers, titanium fibers, and polymeric fibers [32–36]. Previous fiber reinforcement studies can be generally categorized into two groups. Group one focused on short fiber reinforcement in which the fibers had lengths much shorter than the specimen size (e.g., a fiber length of 3 mm versus a specimen length of 25 mm) and were randomly distributed in the matrix, resulting in composites with relatively isotropic properties [25,27,33,35]. Group two focused on continuous fiber reinforcement in which the fibers were nearly as long as the specimen size and were aligned in the matrix in certain directions (e.g., unidirectional) [26,28,30,31,36–38]. The advantage of continuous fiber reinforcement is that the crack resistance is highly enhanced in the direction perpendicular to the fibers. The disadvantage, however, is that the fracture resistance of the composite is anisotropic, in that the crack can propagate easily in the direction parallel to the fibers. In a recent study, a methodology was developed in which fibers with lengths several times longer than the specimen size were randomly mixed with the CPC paste [39]. This resulted in fibers assuming tortuous nonlinear paths in the matrix, combining the advantage of relatively random distribution of short fibers together with the high reinforcement efficacy of continuous fibers. The reinforced CPC composite possessed flexural strength four times, and work-of-fracture (toughness) two orders of magnitude greater than those of the CPC control without fibers. In another study on the relation between fiber strength and composite strength, four different fibers with a wide range of properties were used to reinforce CPC and the composite strength was found to be linearly proportional to the fiber strength [40]. However, the fibers used in these studies [39,40] were stable fibers, not resorbable ones. In addition, no macropores suitable for vascular ingrowth were built into the CPC–fiber composites.

The aim of the present study, therefore, was to incorporate resorbable fibers into CPC so that the set cement would possess (1) significantly increased short-term strength and fracture resistance compared to the unreinforced CPC; and (2) macropores or channels suitable for vascular ingrowth when the fibers are dissolved. Two resorbable fibers with a diameter of 322 μm and different dissolution rates were used. The mechanical properties of the CPC composites were measured as a function of the time immersed in a saline solution. The reinforcement mechanisms and macropores were examined with scanning electron microscopy.

2. Materials and methods

2.1. Specimen fabrication

The CPC powder consisted of a mixture of tetracalcium phosphate [TTCP: $Ca_4(PO_4)_2O$] and dicalcium phosphate anhydrous (DCPA: $CaHPO_4$) [5], with a TTCP : DCPA molar ratio of 1 (BoneSource™, Osteogenics, Winston-Salem, NC). The TTCP powder had a mean size of approximately 12 μm. The DCPA powder had a mean particle size of approximately 1 μm.

Two resorbable fibers were used: Vicryl™ (polyglactin 910, Ethicon, Somerville, NJ), designated as V fiber; and Vicryl Rapide™ (polyglactin 910, Ethicon) designated as VR fiber. According to the manufacturer, the VR fiber had a higher dissolution rate than V fiber. Both fibers were braided with a similar appearance and had an apparent diameter of 322 μm (Fig. 1). To measure the fiber density, fibers of 200 mm length were weighed and the density was calculated as the weight divided by the volume. Both fibers had an apparent density of 0.96 g/cm^3. The fibers were cut with sharp surgical blades into filaments of a length of 8 mm, based on results of previous studies [39,40]. The cut fibers were manually randomized into an irregularly shaped fiber ball [40]. The CPC powder was mixed manually by spatulation with distilled water into a paste. The CPC paste was manually blended with the fiber ball into an irregularly shaped paste ball [40]. The paste ball was then placed into a $3\,mm \times 4\,mm \times 25\,mm$ mold and was lightly pressed into the mold with a spatula. The materials were weighed so that each paste ball slightly overfilled one mold. The composite mixture in the mold was covered with two mechanically clamped glass slides. The assembly was incubated in a humidor with 100% humidity at 37°C for 4 h. The hardened specimen was then demolded, and immediately immersed in a saline

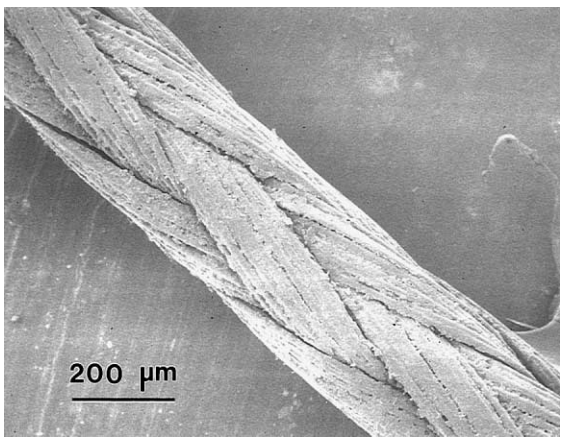

Fig. 1. SEM of a Vicryl Rapide™ fiber showing its braided appearance. The fiber diameter (mean ± SD; $n = 6$) was measured by magnification to be (322 ± 13) μm. Vicryl™ fiber and Vicryl Rapide™ fiber had a similar appearance.

solution (0.9% sodium chloride, Baxter Healthcare Corp., Deerfield, IL) and stored in an oven at 37°C for durations described below. A fiber volume fraction of 25% was used in making the specimens. The fiber volume fraction was calculated as the volume of the fibers in each specimen divided by the total volume of the specimen. The volume of fibers in a specimen was equal to the measured weight of the fibers incorporated into the specimen divided by the fiber density.

Two groups of specimens were made: group one had a mass ratio of CPC powder to water of 2 : 1 for a flowable paste; and group two had a CPC powder : water of 3 : 1 for a thick paste. In each group, three materials were made: CPC without fibers, CPC reinforced with V fiber, and CPC reinforced with VR fiber. Specimens of each material were divided into five batches, each immersed in saline for one of five durations: 1, 7, 14, 28, and 56 d. Six repeats yielded 30 specimens for each of the three materials in each group for a total of 180 specimens.

2.2. Testing

A standard three-point flexural test [41] with a span of 20 mm was used to fracture the specimens at a crosshead speed of 1 mm per minute on a computer-controlled Universal Testing Machine (model 5500R, Instron Corp., MA). The 4 mm × 25 mm surface of the specimen was slightly polished by using silicon carbide papers with grits of 400, 600 and 1200 consecutively, and the specimen was fractured with the polished surface in tension. The following properties were evaluated: flexural strength, flexural modulus, and work-of-fracture (the energy required to fracture the specimen, obtained from the area under the load-displacement curve normalized by the specimen's cross-sectional area) [40]. After the matrices had cracked, many of the fiber-reinforced CPC specimens were still intact, due to fibers bridging the cracks and supporting the applied load. The test was stopped at a maximum crosshead displacement of 2 mm for a consistent calculation of work-of-fracture. After unloading, selected specimens were manually fractured for the examination of fracture surfaces.

A scanning electron microscope (SEM, model JSM-5300, JEOL, Inc., Peabody, MA) was used to observe the specimens. The specimens were sputter coated with gold prior to SEM observations. The fiber-crack interactions, and pullout of fibers were examined to obtain information regarding reinforcement mechanisms. ANOVA was performed to detect significant ($\alpha = 0.05$) effects of material type and immersion days on mechanical properties. Nonparametric Kruskal–Wallis analysis of variance on ranks was performed ($\alpha = 0.05$) in cases of abnormal distribution of or unequal variance in data. Tukey's multiple comparison procedures were used to group and rank the measured values, Dunn's multiple comparison tests were used on data with abnormal distribution or unequal variance, and Dunnett's multiple comparison tests were used to compare to control groups, all at a family confidence coefficient of 0.95.

3. Results

Fig. 2A plots flexural strength versus days of immersion in saline for three materials: CPC control at a powder : water mass ratio of 2 : 1, CPC at the same powder : water ratio reinforced with V fibers, and CPC at the same powder : water ratio reinforced with VR fibers. Each datum is the mean value of six measurements ($n = 6$), with the error bar showing one standard deviation (SD). The strength values of the unreinforced CPC at different immersion days were not significantly different from each other (Dunnett's multiple comparison test; family confidence coefficient = 0.95). For V fiber samples, the strengths at immersion days from 1 to 28 d were not different from each other, but that at 56 d was significantly lower. For VR fiber specimens, the strengths at 1–14 d were not significantly different from each other, but those at 28 and 56 d were significantly lower.

Work-of-fracture is plotted in Fig. 2B for the three materials. The values for V specimens at 1–28 d and those for VR at 1 and 7 d were nearly two orders of magnitude higher than those of CPC control. Fig. 2C plots the elastic modulus of the three materials. Two-way ANOVA showed that none of the materials showed a significant dependence on the immersion days, and there was no significant difference between the materials.

At a higher powder : water mass ratio of 3 : 1, the strength values are plotted in Fig. 3A for CPC control, CPC reinforced with V fibers, and CPC reinforced with VR fibers. The strength values of CPC control at different immersion days were not significantly different from each other (Dunnett's multiple comparison test; family confidence coefficient = 0.95). For V samples, the strengths at immersion days from 1 to 28 d were not significantly different from each other, but that at 56 d was significantly lower. For VR specimens, the strengths at 1–14 d were not significantly different from each other, but those at 28 and 56 d were significantly lower. Strengths of V specimens from 1 to 28 d, and those of VR from 1 to 14 d, were significantly higher than those of the CPC control. Strengths of the three materials at 56 d were not significantly different from each other (Dunnett's multiple comparison test; family confidence coefficient = 0.95).

Work-of-fracture is plotted in Fig. 3B for the three materials at a powder : water ratio of 3 : 1. The values for V specimens at 1–28 d and those for VR at 1 and 7 d were nearly two orders of magnitude higher than those

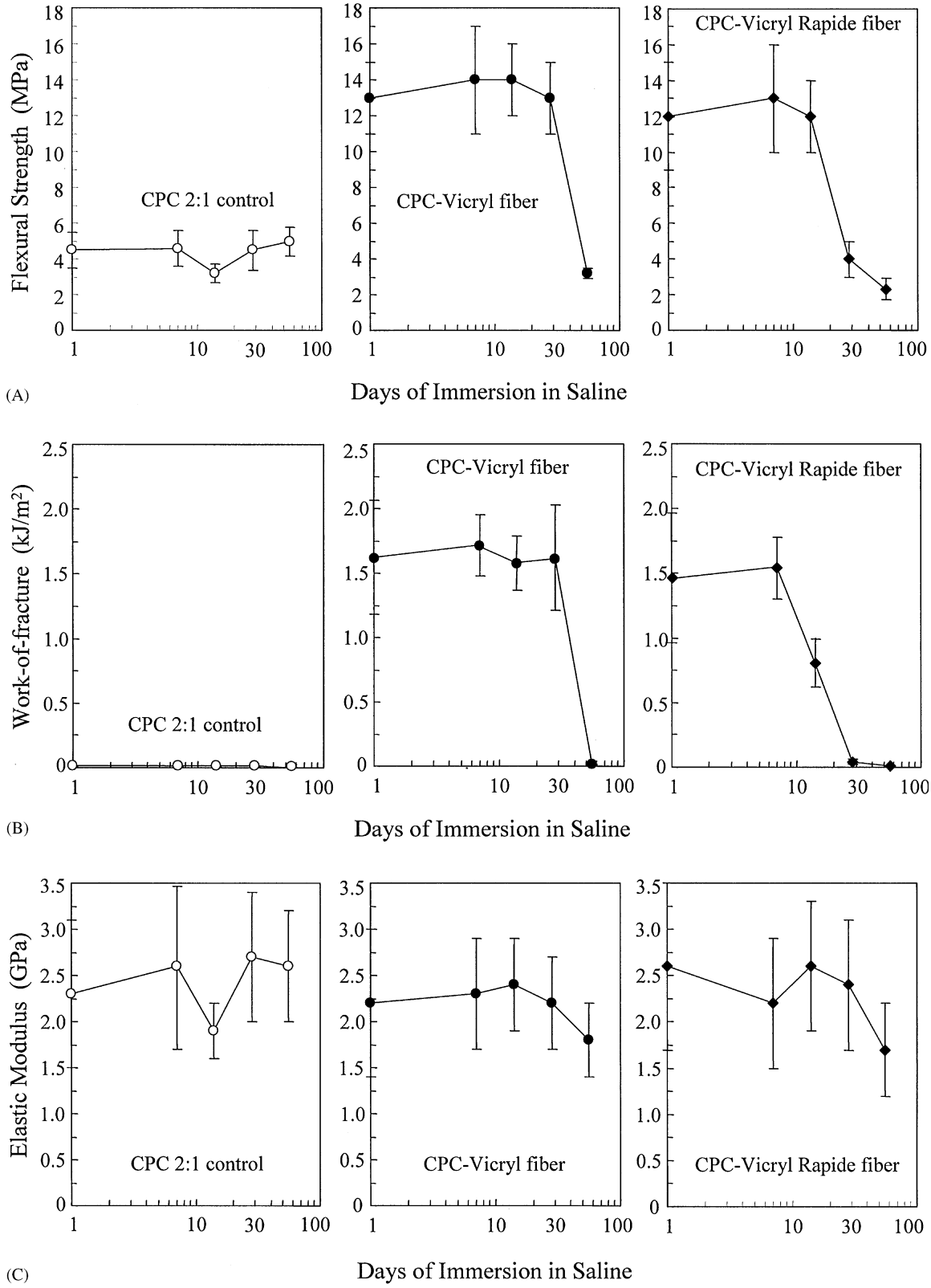

Fig. 2. (A) Flexural strength versus days of immersion in saline for CPC control, CPC-Vicryl™ fiber composite, and CPC-Vicryl Rapide™ fiber composite, all at a CPC powder : water ratio of 2 : 1. Each datum is the mean value of six measurements ($n = 6$), with the error bar showing one standard deviation (SD). (B) Work-of-fracture for CPC control, CPC-Vicryl™ fiber composite, and CPC-Vicryl Rapide™ fiber composite, all at a CPC powder : water ratio of 2 : 1. (C). Elastic modulus for CPC control, CPC-Vicryl™ fiber composite, and CPC-Vicryl Rapide™ fiber composite, all at a CPC powder : water ratio of 2 : 1.

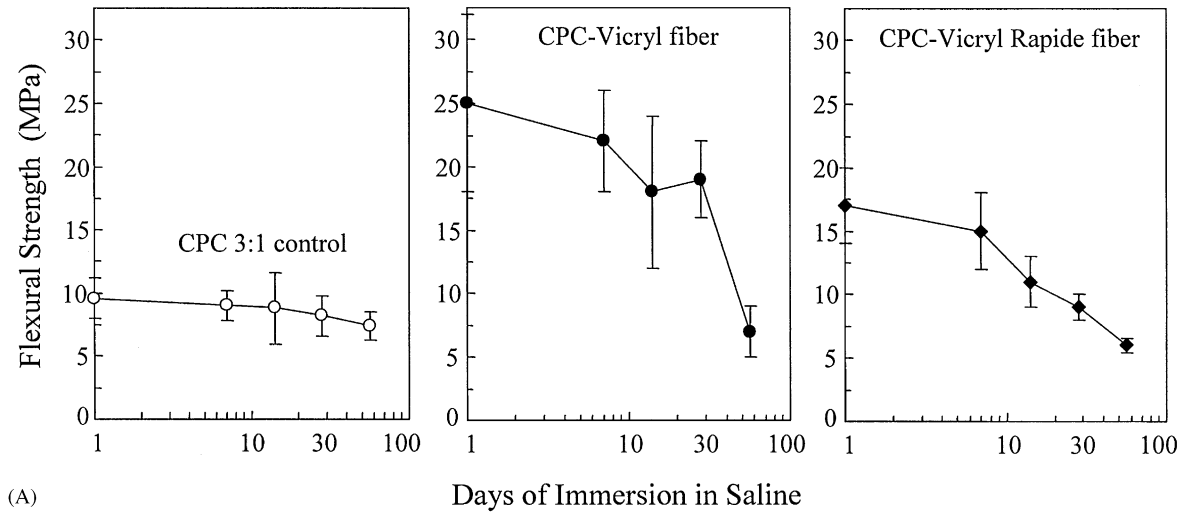

(A)

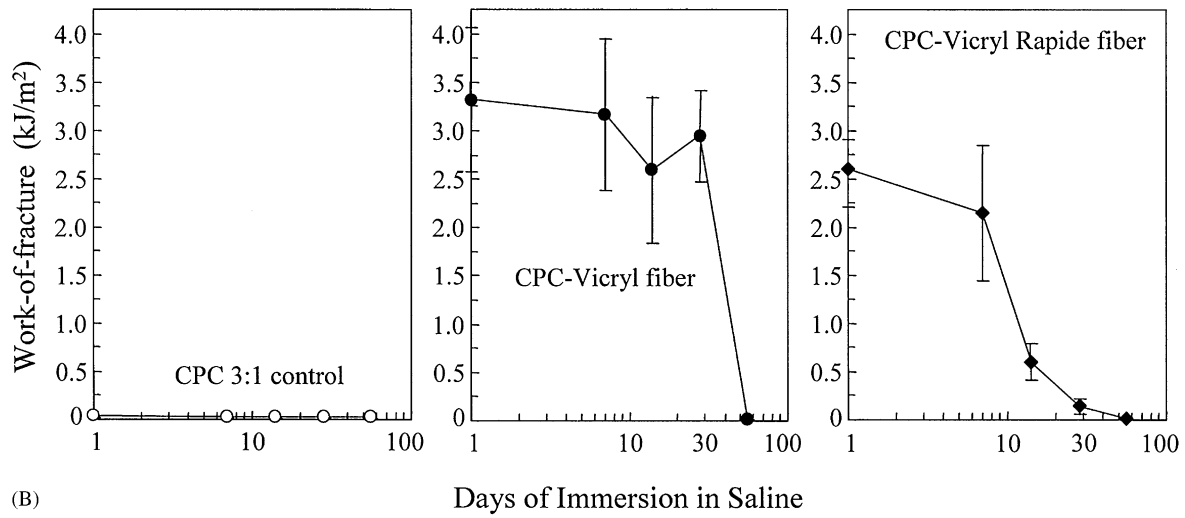

(B)

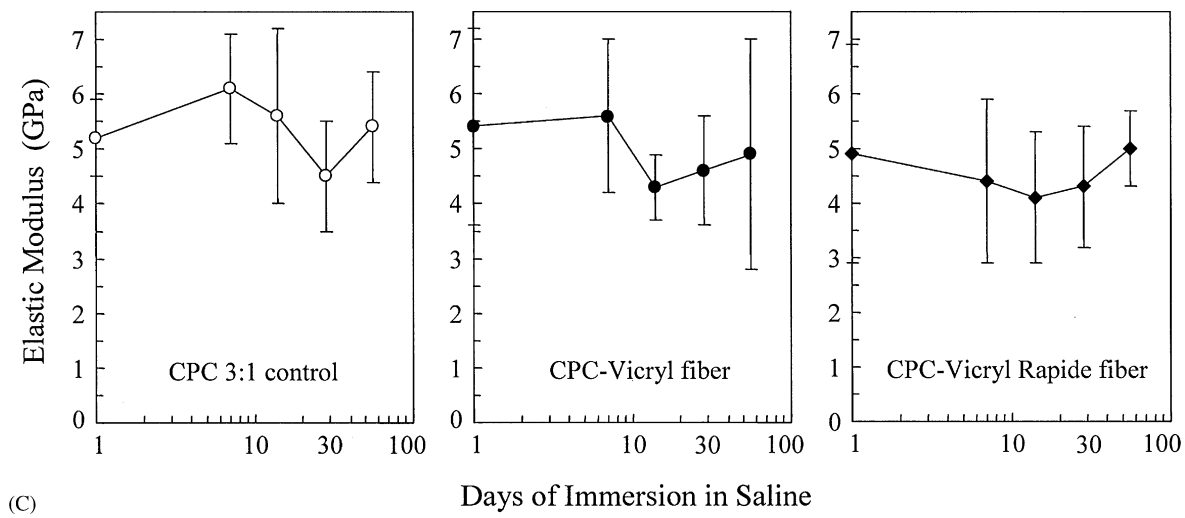

(C)

Fig. 3. (A) At a CPC powder : water mass ratio of 3 : 1, the strength for CPC control, CPC-Vicryl™ fiber composite, and CPC-Vicryl Rapide™ fiber composite. (B) Work-of-fracture for CPC control, CPC-Vicryl™ fiber composite, and CPC-Vicryl Rapide™ fiber composite, at a powder : water ratio of 3 : 1. (C) Elastic modulus for CPC control, CPC-Vicryl™ fiber composite, and CPC-Vicryl Rapide™ fiber composite, at a powder : water ratio of 3 : 1.

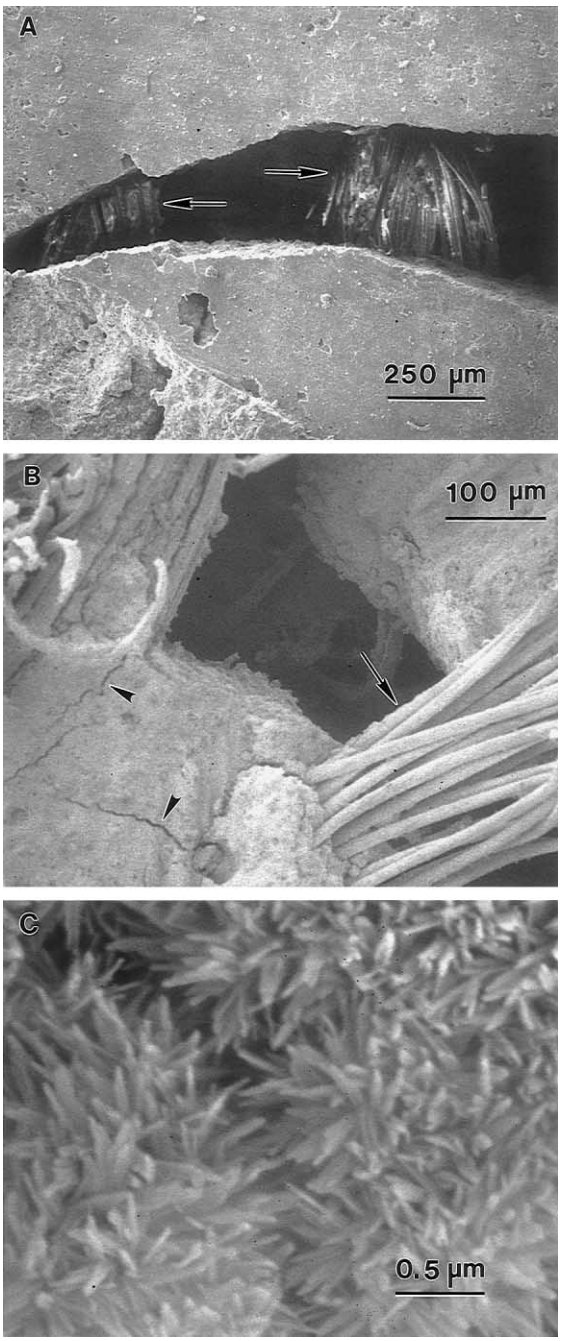

Fig. 4. (A) SEM of a specimen side with the tensile surface on the right, and the crack propagating from right to left. This specimen contained Vicryl Rapide^{TM} (VR) fiber and was immersed in saline for 7 d; the powder : water ratio was 3 : 1. The two VR fibers bridging the crack are indicated by the arrows in (A). (B) The tensile surface of a specimen with Vicryl^{TM} (V) fibers bridging the crack, keeping the multiple-cracked specimen intact. This specimen contained V fiber and was immersed in saline for 7 d; the powder : water ratio was 2 : 1. One braided fiber bundle in (B) appeared to have been separated (long arrow). Numerous microcracks were found in the CPC matrix, examples of which are indicated by the short arrows in (B). (C) Higher magnification SEM showing hydroxyapatite crystallites in the composite specimen, which appeared similar to CPC without fibers, indicating that the fibers had not interfered with hydroxyapatite crystallization.

of CPC control. Fig. 3C plots the elastic modulus of the three materials at a powder : water ratio of 3 : 1. Two-way ANOVA showed that there was no significant difference between immersion days for each material or between materials.

Fig. 4A is a SEM micrograph showing the side of a specimen with the tensile surface on the right, and the crack propagating from right to left. This specimen contained VR fiber and was immersed in saline for 7 d; the powder : water ratio was 3 : 1. The two fibers bridging the crack are indicated by the arrows. Fig. 4B shows the tensile surface of a specimen with fibers bridging the crack; the bridging fibers kept the multiple-cracked specimen intact. This specimen contained V fiber and was immersed in saline for 7 d; the powder : water ratio was 2 : 1. One braided fiber bundle in (B) appeared to have been separated (long arrow) probably due to stresses. Numerous microcracks were found in the matrix, examples of which are indicated by the short arrows in (B). Fig. 4C is a higher magnification SEM

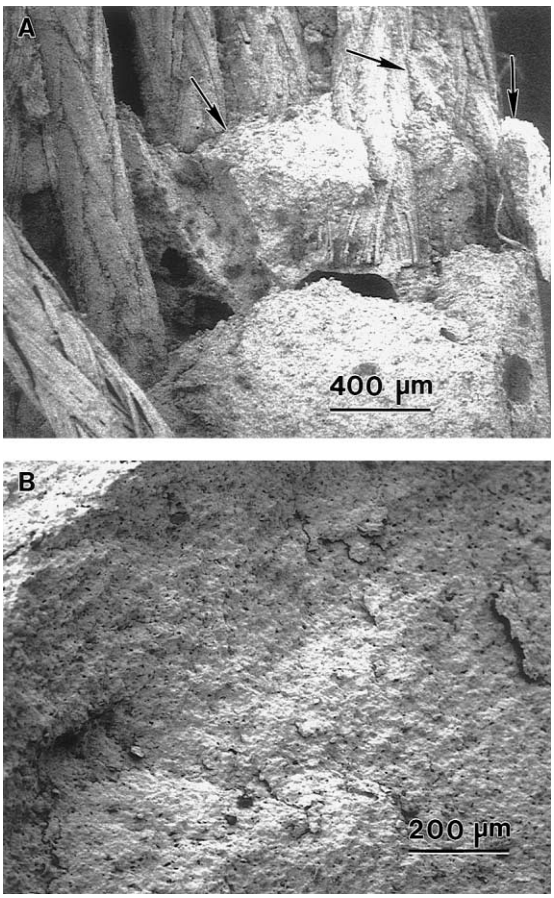

Fig. 5. (A) Fracture surface of composite with fiber pullout and CPC remnants (arrows) adhered to the fibers, showing that the fibers were well dispersed in and wetted by CPC. This specimen had Vicryl Rapide^{TM} fibers and was immersed in saline for 7 d; the powder : liquid ratio was 3 : 1. (B) After the fibers degraded in saline, the fracture surfaces became relatively flat, similar to those of CPC control without fibers.

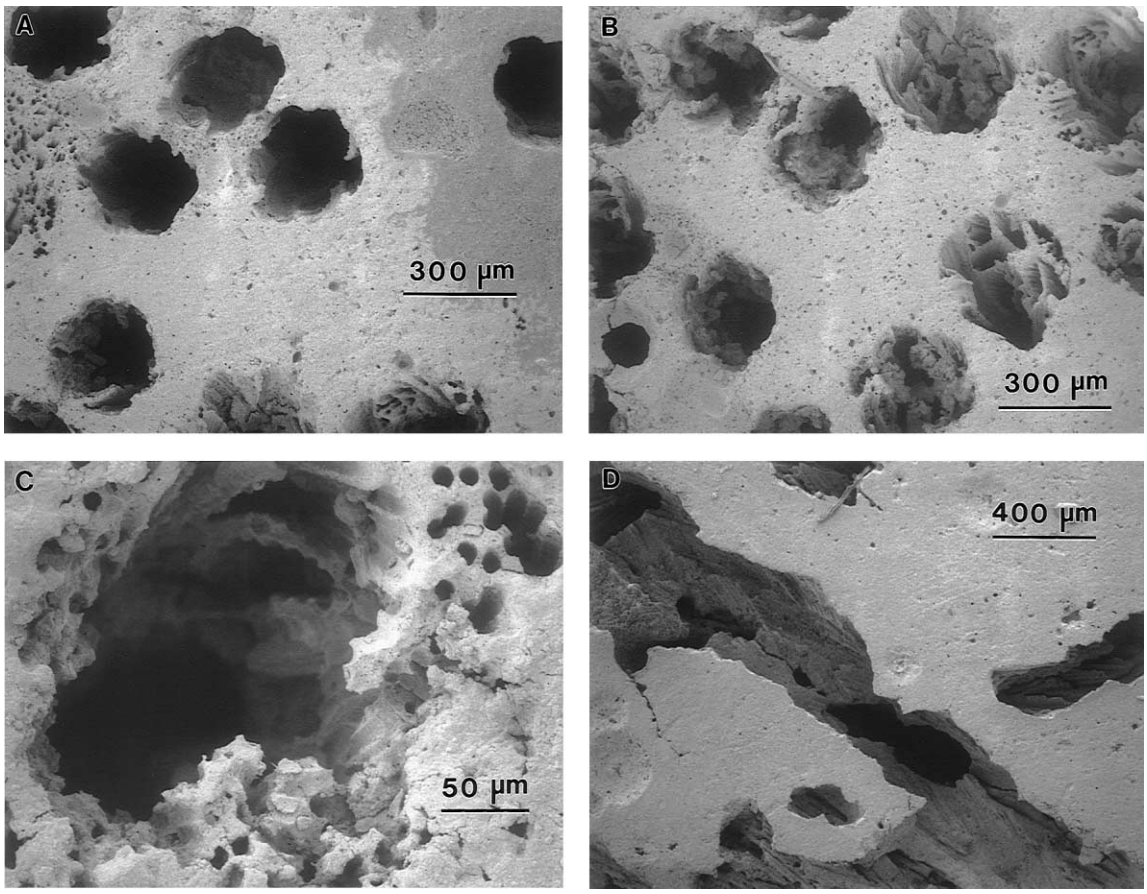

Fig. 6. Macropores were created from fiber dissolution in both V and VR fiber specimens after 12 weeks of immersion. (A) shows holes intercepting the specimen surface. In (B), some holes were not completely empty. A higher magnification of (B) is shown in (C), with a large hole surrounded by a matrix containing small holes. This suggests that, during mixing, the CPC paste may have mingled with the outer layer of the braided fiber bundle, and the small holes in (C) are created from the dissolution of the individual fibers in the bundle. (D) shows macropores nearly parallel to the surface resulting from fiber dissolution.

showing hydroxyapatite crystallites in the composite, which appeared similar to those in CPC without fibers, indicating that incorporating fibers had not interfered with the hydroxyapatite crystallization.

Fig. 5A shows a typical fracture surface of the composite having fiber pullout with remnants of matrix CPC (arrows) adhered to the fibers, demonstrating that the fibers were relatively well dispersed in and wetted by the CPC. This specimen contained VR fibers and was immersed in saline for 7 d; the powder : liquid ratio was 3 : 1. Other composite specimens had similar fracture surfaces before fiber degradation. After the fibers degraded, the fracture surfaces became relatively flat, similar to that of the CPC control without fibers, as is typical for brittle materials. An example of this is shown in Fig. 5B, in which the specimen contained VR fibers and was immersed in saline for 28 d.

No fiber pullout was observed in Fig. 5B, but the lack of macropores suggests that the fibers were still in the matrix and were not completely dissolved yet. The same was observed for V fiber specimens immersed for 56 d. Therefore, the 56 d specimens were further immersed in saline for an additional 28 d (or a total of 12 weeks), and macropores were indeed created from fiber dissolution in both V and VR fiber specimens. Fig. 6A shows holes intercepting the surface of a specimen. Some holes were not completely empty, examples of which are shown in Fig. 6B. A higher magnification of a hole that was not empty is shown in Fig. 6C, with a large hole surrounded by a matrix containing small holes. This suggests that the CPC paste may have mingled with the outer layer of the braided fiber bundle (Fig. 1) during mixing, and the small holes in Fig. 6C are created from the dissolution of the individual fibers in the bundle. Fig. 6D shows macropores that are nearly parallel to the specimen surface resulting from fiber dissolution.

4. Discussion

Previous studies used fibers to reinforce biomedical materials [25–28,30,32–40], including poly(methyl methacrylate) [26,33,37], dental resin composites [28,30,38,42,43], and bone cements [32–36]. Fibers being

used include glass fibers, polymer fibers, titanium fibers and carbon fibers [19,25–28,30–38]. To promote osteoconduction and bone ingrowth, macroporous materials were developed with pore sizes ranging from about 100 μm to about 600 μm. Macroporous calcium phosphate ceramics [44], hydroxyapatite [45], and organic materials [46,47] were produced and investigated for biomedical applications.

A novel methodology was proposed in the present study to combine the superior reinforcement of fibers with the benefit of macropores. Large-diameter resorbable fibers were used to reinforce a self-setting cement to provide the needed short-term strength and toughness, and then dissolved to leave behind macropores suitable for bone ingrowth. Short-term strength tripled, and work-of-fracture increased by nearly 100 times over those of unreinforced CPC. Previous studies showed that the crystallization of hydroxyapatite in CPC continued when the specimens were immersed in water, and CPC was completely converted to hydroxyapatite within about 20 h [8–13]. Therefore, the first measurements in the present study were made after immersion for 1 d, and a time zero value was not measured. A commercially available saline solution was used in this study; in an on-going study on CPC containing resorbable fibers of different lengths and volume fractions, the specimens were immersed in a simulated physiological solution. Vicryl polyglactin 910 fibers were used in this study because a previous clinical study showed that these fibers had significant potential as an absorbable dural substitute with minimal inflammatory reaction [48]. The duration of reinforcement for CPC depended on the type of resorbable fibers. The V fiber composite immersed in the saline solution maintained its strength to 4 weeks, while the VR fibers to 2 weeks of immersion, consistent with information on fiber duration from the manufacturer. These fibers produced macropores of about 300 μm in diameter. Other types of resorbable fibers can be used to tailor dissolution rate and macropore size suitable for specific applications. One recent study used a suture mesh on the tensile side of the specimen to achieve significantly higher work-of-fracture; no macropores were produced in the bulk of CPC as the thin mesh was limited to one surface of the specimen [19]. The present study mixed the CPC paste with resorbable fibers of 8 mm length to a volume fraction of 25%. Further studies are underway to increase the volume fraction of macropores by using higher fiber volume fractions. An on-going study showed that with a shorter fiber length of 3 mm, a higher volume fraction of 35% fibers were readily mixed with CPC into a cohesive paste.

The fibers appeared to be well wetted by the CPC matrix, manifested by them being well surrounded by CPC (Fig. 4B) and by CPC pieces being adhered to the pulled-out fibers (Fig. 5A). The relatively rough surfaces of the braided fibers (Fig. 1) probably enhanced the interlocking of the fibers in the matrix. The mechanisms of reinforcement in the present study appeared to be (1) fibers bridging the crack to resist its further opening and propagation (Figs. 4A and B); (2) multiple cracking of matrix consuming the applied work in creating new surfaces (Fig. 4B showing some of the microcracks in the matrix); and (3) frictional sliding and stretching of fibers during pullout (Fig. 5A). Enamel rods in tooth behave in a way similar to fibers by deflecting and resisting cracks [49], and toughening mechanisms of bridging and pullout have been observed in other ceramic matrix composites [29,50,51].

Besides fiber effects, the CPC matrix also significantly influenced the composite properties. For example, when the powder : water ratio was increased from 2 : 1 to 3 : 1, the matrix strength was increased by approximately 5 MPa (1 d immersion); however, the strength of the CPC-Vicryl composite was increased by 12 MPa. A more dramatic effect was seen in work-of-fracture. When the powder : water ratio was increased from 2 : 1 to 3 : 1, the work-of-fracture of the matrix CPC was increased by approximately 0.01 kJ/m^2; that of CPC-Vicryl composite was increased by 1.67 kJ/m^2, two orders of magnitude times the difference observed in matrices alone.

The present study focused on the reinforcement of CPC with two types of resorbable large-diameter fibers for short-term strength and macroporosity. The three-fold increase in strength and nearly two orders of magnitude increase in work-of-fracture (toughness) of the fiber-reinforced calcium phosphate cement may help extend the medical and dental applications into the repair of larger defects, use in stress-bearing locations, and reconstructive treatments for thin bones. In addition, the macropores in CPC may help new bone formation and implant dissolution/resorption. The novel methodology of combining the superior reinforcement of fibers with macropores suitable for vascular ingrowth could be applied to other biomaterials.

Acknowledgements

The authors are grateful to Dr. F.C. Eichmiller for discussions and help in statistical analysis, and to Drs. G.E. Schumacher, J.M. Antonucci, J.R. Kelly, S. Takagi and L.C. Chow for discussions. This study was supported by USPHS NIDCR Grant R29 DE12476, NIST, and the ADAHF.

Disclaimer

Certain commercial materials and equipment are identified in this paper to specify experimental

procedures. In no instance does such identification imply recommendation by NIST or the ADA Health Foundation or that the material identified is necessarily the best available for the purpose.

References

[1] Osborn JF, Newesely H. The materials science of calcium phosphate ceramics. Biomaterials 1980;1:108–11.

[2] Hench LL. Bioceramics. J Am Ceram Soc 1998;81(7):1705–28.

[3] Suchanek W, Yoshimura M. Processing and properties of hydroxyapatite-based biomaterials for use as hard tissue replacement implants. J Mater Res 1998;13(1):94–117.

[4] Monma H, Goto M, Konmura T. Effect of additives on hydration and hardening of tricalcium phosphate. Gypsum Lime 1984; 188:11–6.

[5] Brown WE, Chow LC. In: Brown PW, editor. A new calcium phosphate water setting cement. Cements research progress. Westerville, OH: American Ceramic Society, 1986. p. 352–79.

[6] Ginebra MP, Fernandez E, De Maeyer EAP, Verbeeck RMH, Boltong MG, Ginebra J, Driessens FCM, Planell JA. Setting reaction and hardening of an apatite calcium phosphate cement. J Dent Res 1997;76(4):905–12.

[7] Constantz BR, Barr BM, Ison IC, Fulmer MT, Baker J, McKinney L, Goodman SB, Gunasekaren S, Delaney DC, Ross J, Poser RD. Histological, chemical, and crystallographic analysis of four calcium phosphate cements in different rabbit osseous sites. J Biomed Mater Res (Appl Biomater) 1998;43: 451–61.

[8] Friedman CD, Costantino PD, Takagi S, Chow LC. BoneSource™ hydroxyapatite cement: a novel biomaterial for craniofacial skeletal tissue engineering and reconstruction. J Biomed Mater Res (Appl Biomater) 1998;43:428–32.

[9] Miyamoto Y, Ishikawa K, Takechi M, Toh T, Yuasa T, Nagayama M, Suzuki K. Histological and compositional evaluations of three calcium phosphate cements when implanted in subcutaneous tissue immediately after mixing. J Biomed Mater Res (Appl Biomater) 1999;48:36–42.

[10] Chow LC, Takagi S, Ishikawa K. Formation of hydroxyapatite in cement systems. In: Brown PW, Constanz B, editors. Material Research Society Proceedings. San Francisco, CA: CRC Press, 1993.

[11] Fukase Y, Eanes ED, Takagi S, Chow LC, Brown WE. Setting reactions and compressive strengths of calcium phosphate cement. J Dent Res 1990;69:1852–6.

[12] Costantino PD, Friedman CD, Jones K, Chow LC. Hydroxyapatite cement: I. Basic chemistry and histologic properties. Arch Otolaryngol Head Neck Surg 1991;117:379–84.

[13] Friedman CD, Costantino PD, Jones K, Chow LC. Hydroxyapatite cement: II. Obliteration and reconstruction of the cat frontal sinus. Arch Otolaryngol Head Neck Surg 1991;117:385–9.

[14] Miyamoto Y, Ishikawa K, Fukao K, Sawada M, Nagayama M, Kon M, Asaoka K. In vivo setting behavior of fast-setting calcium phosphate cement. Biomaterials 1995;16:855–60.

[15] Costantino PD, Friedman CD. Synthetic bone graft substitutes. Otolaryngol Clin North Am 1994;27:1037–74.

[16] Ishikawa K, Takagi S, Chow LC, Ishikawa Y. Properties and mechanisms of fast setting calcium phosphate cements. J Mater Sci: Mater Med 1995;6:528–33.

[17] Shindo ML, Costantino PD, Friedman CD, Chow LC. Facial skeletal augmentation using hydroxyapatite cement. Arch Otolaryngol Head Neck Surg 1993;119:185–90.

[18] Costantino PD, Friedman CD, Jones K, Chow LC, Sisson GA. Experimental hydroxyapatite cement cranioplasty. Plast Reconstr Surg 1992;90:174–91.

[19] von Gonten AS, Kelly JR, Antonucci JM. Load-bearing behavior of a simulated craniofacial structure fabricated from a hydroxyapatite cement and bioresorbable fiber-mesh. J Mater Sci: Mater Med 2000;11:95–100.

[20] Chohayeb AA, Chow LC, Tsaknis P. Evaluation of calcium phosphate as a root canal sealer-filler material. J Endodont 1987;13:384–7.

[21] Sugawara A, Nishiyama M, Kusama K, Moro I, Nishimura S, Kudo I, Chow LC, Takagi S. Histopathological reaction of calcium phosphate cement. Dent Mater J 1992;11:11–6.

[22] Sugawara A, Chow LC, Takagi S, Chohayeb H. In vitro evaluation of the sealing ability of a calcium phosphate cement when used as a root canal sealer-filler. J Endodon 1990;16:162–5.

[23] Dickens-Venz SH, Takagi S, Chow LC, Bowen RL, Johnston AD, Dickens B. Physical and chemical properties of resin-reinforced calcium phosphate cements. Dent Mater 1994; 10:100–6.

[24] Matsuya Y, Antonucci JM, Matsuya S, Takagi S, Chow LC. Polymeric calcium phosphate cements derived from poly(methyl vinyl ether-maleic acid). Dent Mater 1996;12:2–7.

[25] Saha S, Pal S. Improvement of mechanical properties of acrylic bone cement by fiber reinforcement. J Biomech 1984;17:467–78.

[26] Pourdeyhimi B, Robinson HH, Schwartz P, Wagner HD. Fracture toughness of Kevlar 29/poly(methyl methacrylate) composite materials for surgical implantations. Ann Biomed Eng 1986;14:277–94.

[27] Pourdeyhimi B, Wagner HD. Elastic and ultimate properties of acrylic bone cement reinforced with ultra-high-molecular-weight polyethylene fibers. J Biomed Mater Res 1989;23:63–80.

[28] Ladizesky NH, Cheng YY, Chow TW, Ward IM. Acrylic resin reinforced with chopped high performance polyethylene fiber-properties and denture construction. Dent Mater 1993;9: 128–35.

[29] Lawn BR. Fracture of brittle solids. London: Cambridge University Press, 1993 [chapter 8].

[30] Goldberg AJ, Burstone CJ, Hadjinikolaou I, Jancar J. Screening of matrices and fibers for reinforced thermoplastics intended for dental applications. J Biomed Mater Res 1994;28:167–73.

[31] Xu HHK, Ostertag CP, Braun LM, Lloyd IK. Short-crack mechanical properties and failure mechanisms of Si_3N_4-matrix/SiC-fiber composites. J Am Ceram Soc 1994;77:1889–96.

[32] Topoleski LDT, Ducheyne P, Cuckler JM. The fracture toughness of titanium-fiber-reinforced bone cement. J Biomed Mater Res 1992;26:1599–617.

[33] Topoleski LDT, Ducheyne P, Cuckler JM. The effects of centrifugation and titanium fiber reinforcement on fatigue failure mechanisms in poly(methyl methacrylate) bone cement. J Biomed Mater Res 1995;29:299–307.

[34] Kettunen J, Makela A, Miettinen H, Nevalainen T, Heikkila M, Tormala P, Rokkanen P. The effect of an intramedullary carbon-fiber-reinforced liquid crystalline polymer implant on bone: an experimental study on rabbits. J Biomed Mater Res 1998;42: 407–11.

[35] Schreiber CK. The clinical application of carbon fiber/polymer denture bases. Br Dent J 1974;137:21–2.

[36] Pal S, Saha S. Stress relaxation and creep behavior of normal and carbon fiber reinforced acrylic bone cement. Biomaterials 1982; 3:93–6.

[37] Ruyter IE, Ekstrand K, Bjork N. Development of carbon/graphite fiber reinforced poly(methyl methacrylate) suitable for implant-fixed dental bridges. Dent Mater 1986;2:6–9.

[38] Malquarti G, Berruet RG, Bois D. Prosthetic use of carbon fiber-reinforced epoxy resin for esthetic crowns and fixed partial dentures. J Prosthet Dent 1990;63:251–7.

[39] Xu HHK, Eichmiller FC, Barndt PR. Effects of fiber length and volume fraction on the reinforcement of calcium phosphate cement. J Mater Sci: Mater Med 2001;12:57–65.
[40] Xu HHK, Eichmiller FC, Giuseppetti AA. Reinforcement of a self-setting calcium phosphate cement with different fibers. J Biomed Mater Res 2000;52:107–14.
[41] American Society for Testing and Materials. ASTM F417-78: standard test method for flexural strength of electrical grade ceramics. Philadelphia, PA: ASTM, 1984.
[42] Xu HHK, Martin TA, Antonucci JM, Eichmiller FC. Ceramic whisker reinforcement of dental composite resins. J Dent Res 1999;78:706–12.
[43] Xu HHK. Dental composite resins containing silica-fused ceramic single-crystalline whiskers with various filler levels. J Dent Res 1999;78:1304–11.
[44] Bouler JM, Trécant M, Delécrin J, Royer J, Passuti N, Daculsi G. Macroporous biphasic calcium phosphate ceramics: influence of five synthesis parameters on compressive strength. J Biomed Mater Res 1996;32:603–9.
[45] Chang BS, Lee CK, Hong KS, Youn HJ, Ryu HS, Chung SS, Park KW. Osteoconduction at porous hydroxyapatite with various pore configurations. Biomater 2000;21:1291–8.
[46] Madihally SV, Matthew HWT. Porous chitosan scaffolds for tissue engineering. Biomater 1999;20:1133–42.
[47] Zhang R, Ma PX. Poly(α-hydroxyl acids)/hydroxyapatite porous composites for bone-tissue engineering. I. Preparation and morphology. J Biomed Mater Res 1999;44:446–55.
[48] Maurer PK, McDonald JV. Vicryl (polyglactin 910) mesh as a dural substitute. J Neurosurg 1985;63:448–52.
[49] Xu HHK, Smith DT, Jahanmir S, Romberg E, Kelly JR, Thompson VP, Rekow ED. Indentation damage and mechanical properties of human enamel and dentin. J Dent Res 1998;77:472–80.
[50] Xu HHK, Ostertag CP, Fuller ER, Braun LM, Lloyd IK. Fracture resistance of SiC-fiber-reinforced Si_3N_4 composites at ambient and elevated temperatures. J Am Ceram Soc 1995;78:698–704.
[51] Xu HHK, Ostertag CP, Braun LM, Lloyd IK. Effects of fiber volume fraction on mechanical properties of SiC-fiber/Si_3N_4-matrix composites. J Am Ceram Soc 1994;77:1897–990.